

Warming Trend of the Indian Ocean SST and Indian Ocean Dipole from 1880 to 2004*

CHIE IHARA, YOCHANAN KUSHNIR, AND MARK A. CANE

Lamont-Doherty Earth Observatory, Columbia University, Palisades, New York

(Manuscript received 9 March 2007, in final form 14 September 2007)

ABSTRACT

The state of the Indian Ocean dipole representing the SST anomaly difference between the western and southeastern regions of the ocean is investigated using historical SST reconstructions from 1880 to 2004. First, the western and eastern poles of the SST-based dipole mode index are analyzed separately. Both the western and eastern poles display warming trends over this period, particularly after the 1950s. The western pole tends to be anomalously colder than the eastern pole from 1880 to 1919, whereas in the interval 1950–2004 the SST anomalies over the western pole are comparable to those over the eastern pole though there are occasional outliers where the eastern pole is anomalously colder than the western pole.

The tendencies of the occurrences of positive and negative dipole events in September–November show three distinct regimes during the period analyzed. In 1880–1919, negative dipole events associated with La Niña events occur more frequently than positive events. In 1920–49, some weak positive events occur relatively independently of El Niño events over the Pacific. The period of 1960–2004 is characterized by strong and frequent occurrences of positive events associated with El Niño events.

1. Introduction

Though there had been earlier studies of the interannual variability of the zonal sea surface temperature (SST) gradient over the equatorial Indian Ocean (e.g., Saha 1970; Reverdin et al. 1986), after Saji et al. (1999) and Webster et al. (1999) discovered a phenomenon that includes both atmospheric and oceanic variables and called it the Indian Ocean dipole mode or Indian Ocean zonal mode, the number of studies related to this phenomenon increased dramatically. According to Saji et al. (1999), the Indian Ocean dipole mode is characterized by the anomalous west–east SST gradient accompanying zonal wind anomalies over the equatorial Indian Ocean; during positive events the western Indian Ocean is warmer than normal; the southeast Indian Ocean, off of Sumatra, is colder than normal; and the anomalous easterlies appear around the central equatorial Indian Ocean. They also found that the di-

pole events were seasonally phase locked: an event started in May–June, matured in October, and decayed in boreal winter. Li et al. (2003) suggested that a thermodynamic air–sea interaction over the southeast Indian Ocean explained this feature of the dipole mode. In boreal summer, the anomalous wind induced by the cooling over this region enhances the mean southeasterly flow over the equatorial Indian Ocean, which in turn enhances the surface evaporation, vertical mixing, and coastal upwelling off of Sumatra. This sequence of factors further cools the southeast Indian Ocean. When the mean flow changes from southeasterly to northwesterly in boreal winter, the same anomalous flow weakens the mean flow and dampens the cooling over the southeast Indian Ocean. The thermodynamic air–sea interaction works as a positive feedback in boreal summer but also as a negative feedback in boreal winter. Thus, Li et al. (2003) claimed that feedback mechanisms that were dependent on the season could explain why dipole events developed in boreal summer and decayed in boreal winter.

There is some controversy over whether the dipole mode events are independent of El Niño–Southern Oscillation (ENSO) and are inherent to the Indian Ocean (Allan et al. 2001). Saji et al. (1999) and Webster et al. (1999) claimed that the events could occur without ENSO, pointing to 1961, a year when a strong positive

* Lamont-Doherty Earth Observatory Contribution Number 7107.

Corresponding author address: Chie Ihara, Lamont-Doherty Earth Observatory, Columbia University, 61 Route 9W, Palisades, NY 10964-8000.
E-mail: cihara@ldeo.columbia.edu

dipole event occurred without El Niño. Lau and Nath (2004) suggested that in addition to ENSO, the southern annular mode (SAM) could be one of the triggers of the Indian Ocean events based on output from a coupled general circulation model simulation. Fischer et al. (2004) concurred with the findings of Lau and Nath and in their study, the cold SST in the southeast tropical Indian Ocean accompanying the strong Mascarene high triggered the northward penetration of the southeast trades over the equatorial Indian Ocean, which was favorable for the development of the dipole mode.

As a mode of climate variability in the Indian Ocean, the impacts of the Indian Ocean dipole on the global climate are also examined. Previous papers have addressed the connection of the dipole mode to the climate of India (Ashok et al. 2001, 2004b; Ihara et al. 2008), East Africa (Clark et al. 2003; Behera et al. 2005), the extratropics (Guan and Yamagata 2003; Saji and Yamagata 2003), and the East Asian monsoon (Kripalani et al. 2005). Discussions of the definition and physical mechanisms of the Indian Ocean dipole mode, particularly its relation to ENSO, are on going. However, it may now be fair to say that its existence and scientific importance are becoming accepted within the scientific community.

The Indian Ocean dipole, defined by a zonal SST gradient, is known to have decadal to multidecadal variability (e.g., Annamalai et al. 2005; Ashok et al. 2004a; Chang et al. 2006; Kripalani and Kumar 2004; Tozuka et al. 2007). Annamalai et al. (2005) suggested a connection between the strong dipole events in the 1960s and 1990s and the Pacific decadal variability. Ashok et al. (2004a) demonstrated the existence of 8–25-yr low-frequency signals of the Indian Ocean dipole. Tozuka et al. (2007) pointed out asymmetric occurrences of positive and negative dipole mode events over a period that spanned about 10 yr and called it the decadal modulation of interannual Indian Ocean dipole mode events. In terms of multidecadal variability, Kripalani and Kumar (2004) found that the Indian Ocean dipole was in a negative phase in the period between 1880 and 1920 and was in a positive phase in the period between 1960 and 2000. Our interest here is in the multidecadal variability, as found in Kripalani and Kumar (2004), that is, irregular occurrences of negative (in the late nineteenth century and the early twentieth century) and positive events (in the second half of the twentieth century). Thus, the time scale of the change focused upon in this study is about a century—longer than earlier studies on decadal variations.

We are particularly interested in multidecadal variability since this secular change in the occurrences of

positive and negative events between the first and second halves of the twentieth century is conceivably related to the warming trend over the Indian Ocean during this period. The warming SST over the Indian Ocean has been addressed by many earlier papers (Allan et al. 1995; Terray and Dominiak 2005, and references therein). Allan et al. (1995) examined the conditions of the Indian Ocean from 1900 to 1983 in boreal winter and found that overall, the SST displayed a warming trend. Terray and Dominiak (2005) showed that the entire Indian Ocean basin demonstrated substantial warming after the 1976–77 climate regime shift over the Pacific Ocean. These changes may in part be natural variation, or may be the local manifestation of global warming caused by the anthropogenic greenhouse gases and aerosols. If we suppose these warming trends are homogeneous in space, the anomalous SST gradient over the equatorial Indian Ocean should remain the same. But if not, these trends could affect the strength of both positive and negative dipole events, and may be related to the multidecadal variability of the Indian Ocean dipole mode events. Thus, it is of great importance to delineate the relationship between the SST anomalies in the western and eastern poles of the dipole mode over the long term in consideration of the warming trend over these regions.

In this paper, we investigate the state of the Indian Ocean dipole as represented by SST anomalies from 1880 to 2004, and reveal that a change occurred in the relationship between SST anomalies over the western and eastern poles of the Indian Ocean dipole. The change in the characteristics of the same positive and negative dipole events defined by their index is also delineated during this long-term period. Since the weak warming trend in the early half of the twentieth century compared to the intense warming after the mid-1970s is reported in the global mean annual land surface air temperature (e.g., Jones et al. 2006), we infer that warming trend of the Indian Ocean from 1880 to 2004 may not be monotonic and thus we try to take into account the different regimes of the warming trend in our analysis. Our work is different from that of Ashok et al. (2003) in that they examined the long-term state of the Indian Ocean dipole because the trend of the dipole mode index was linearly removed in their analysis. Kripalani and Kumar (2004) pointed out the multidecadal variability of the Indian Ocean dipole but the state of the Indian Ocean dipole in the warming trend, particularly the relationship between the western and eastern poles, was not fully examined there. Section 2 is devoted to the description of the datasets used in this study. In section 3, we discuss the warming trends over the western and eastern poles separately and present

their relationships in three different periods. In section 4, we demonstrate the changes within the occurrences of positive and negative events and the Indo-Pacific SST patterns associated with these events. Section 5 is devoted to a summary and discussions.

2. Data descriptions

Monthly, $1^\circ \times 1^\circ$ gridded SST anomalies from 1880 to 2004 are obtained from Smith and Reynolds (2004), the so-called National Oceanic and Atmospheric Administration/National Climatic Data Center (NOAA/NCDC) Extended Reconstructed SST (ERSST) dataset, version 2. For comparison, monthly $4^\circ \times 4^\circ$ gridded SST anomalies from 1880 to 2004 obtained from Kaplan et al. (2003) are also used. SST anomaly data are averaged over 3 months by season: December–February, March–May, June–August, and September–November. The climatology in this study is defined as the mean SST during the period between 1880 and 2004 to address the state of the Indian Ocean SST, including the trend component.

Different methods are used for the reconstructions of the ERSST and Kaplan SST datasets. Smith and Reynolds (2003) separated low- and high-frequency variabilities and reconstructed the high-frequency variability by the projection method. Kaplan et al. (2003) used an optimal smoothing method assuming the stationarity of the data in the modern base period and dealt with all frequencies in the same manner. Thus, there is a criticism that the warming trend of SST over the twentieth century is underestimated in the Kaplan SST data while it more effectively captures the large-scale structures of SSTs (Hurrell and Trenberth 1999). However, the results we are going to show do not differ remarkably between the ERSST data and the Kaplan SSTs even though some discrepancies are expected between these two SST datasets.

The data prior to the 1880s are not included in our study to avoid the uncertainties that have been reported to affect this early period (Kaplan et al. 1998; Smith and Reynolds 2003). The equatorial Indian Ocean displays rich data coverage from the early period of analysis compared to the equatorial eastern Pacific. The Comprehensive Ocean–Atmosphere Data Set (COADS) SSTs, from which the ERSST results are derived (Slutz et al. 1985), show that, roughly speaking, the tropical Indian Ocean has twice the number of observations as the equatorial eastern Pacific from the late nineteenth century throughout the 1960s, except for the 1940s when the data coverage was sparse in the both oceans. Thus, it can be said that the tropical Indian Ocean is the region that offers reliable SST datasets

even in the late nineteenth century and the early twentieth century. There may be a concern about the data quality before the 1950s compared to the data quality after the 1950s in the tropical Indian Ocean, but the number of observations in the equatorial Indian Ocean before the 1950s is comparable or sometimes larger to that from the 1950s throughout the 1970s, except for three short periods: 1880–1900, just before 1920, and the time of World War II, 1940–45. In 1880–1900, the number of observations of the tropical Indian Ocean is generally about half of that from the 1950s throughout the 1970s. But in the short periods just before 1920 and 1940–45, the number of observations of the tropical Indian Ocean drops steeply compared to the preceding period. The overall tendency of the data coverage is almost the same for the data from version 5 of the Met Office Historical Sea Surface Temperature (MOHSST5) dataset, from which the Kaplan SST data are derived (Kaplan et al. 1998). We judge that though the SST data before the 1950s are not as good as the SST data from the 1950s throughout the 1970s because of these short data-sparse periods, we still believe that the historical SST datasets in the early period are reliable enough to conduct research on the secular change of the equatorial Indian Ocean SST. We use caution with the results based on the data-sparse periods mentioned above and we compensate for the limitations of the data quality during these periods; thus, we confirm our results by using the two new and different SST reconstructions.

3. Western and eastern poles of the Indian Ocean dipole events

a. Trends in the SST anomalies over the western and eastern poles

The Indian Ocean dipole events are represented by the dipole mode index obtained by the SST anomaly difference over the western Indian Ocean and the southeast Indian Ocean (hereafter referred to as SSTDMI). The western pole of SSTDMI is located at the western equatorial Indian Ocean (hereafter referred to as WEIO) representing SST anomalies averaged in the box from 10°S to 10°N and from 50° to 70°E (Fig. 1). The eastern pole of SSTDMI is located at the eastern equatorial Indian Ocean (hereafter referred to as EEIO) representing SST anomalies averaged in the box from 10°S to 0° and from 90° to 110°E (Fig. 1). Figure 2 shows the 10-yr running means of the seasonal WEIO and EEIO from 1880 to 2004; the top panel corresponds to WEIO and EEIO obtained from the ERSST data, and the bottom panel corresponds to the results obtained from the Kaplan SST data. Both the

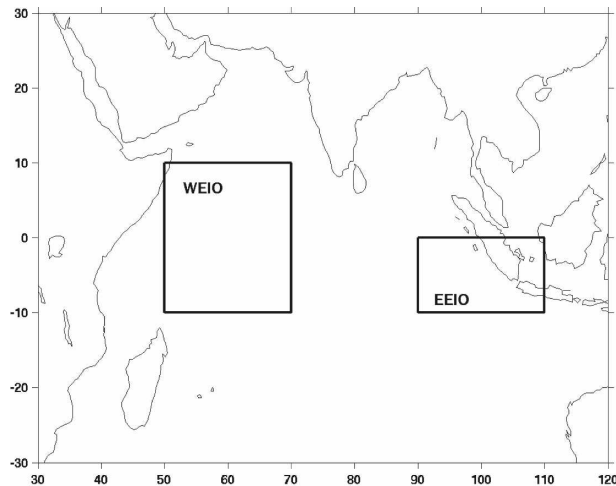


FIG. 1. Locations of the western and eastern poles of the SSTDMI. The western pole represents the box from 10°S to 10°N and from 50° to 70°E, and the eastern pole represents the box from 10°S to 0° and from 90°E to 110°E.

ERSST and Kaplan SST datasets display similar trends over these regions for the entire period. Except around the 1940s, the overall trend is warming during the twentieth century. The time series shown here implies the existence of three different regimes in the warming trend of the Indian Ocean SST anomalies. The first is

from 1880 to 1919 when the warming trend of the EEIO seems to be less prominent when compared to the later period. The second period is from 1920 to 1949 when both WEIO and EEIO exhibit warming followed by a brief interval of steep cooling. The third period is from 1950 to 2004 when the both WEIO and EEIO demonstrate the strong warming trend, $\sim 0.5^{\circ}\text{C}$ over 50 yr. The strong warming after the 1950s over WEIO and EEIO was also pointed out by Kulkarni et al. (2007).

The SST warming trend presented in these figures cannot be explained only by the local climate variability over the Indian Ocean region. It is rather a global phenomenon since the warming trend in the early twentieth century, the slight cooling around the 1940s, and the subsequent warming after the mid-1970s are also seen in the global mean annual land surface air temperature (e.g., Jones et al. 2006) and in several other ocean basins (Kaplan et al. 2003; Smith and Reynolds 2004).

There is a difference between the two SST datasets in the 1930s and 1940s, when data are sparse; the western pole tends to be slightly, anomalously warmer than the eastern pole in the ERSST but not in Kaplan SST data. In the early twentieth century, the warming trend seems to start over both poles, but in both the ERSST and Kaplan SST data, the warming trend over the western pole is found in the 1910s whereas it does not seem to appear over the eastern pole until after the 1920s.

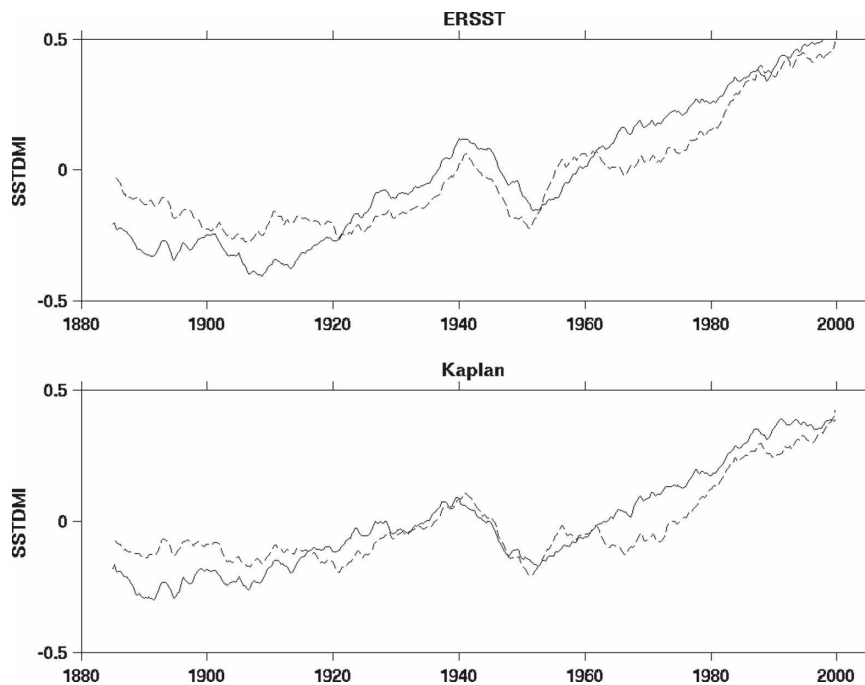


FIG. 2. The 10-yr running means of WEIO and EEIO from 1880 to 2004. The solid lines indicate WEIO and the dashed lines indicate EEIO. Indices are obtained from (top) the ERSST and (bottom) the Kaplan SST data.

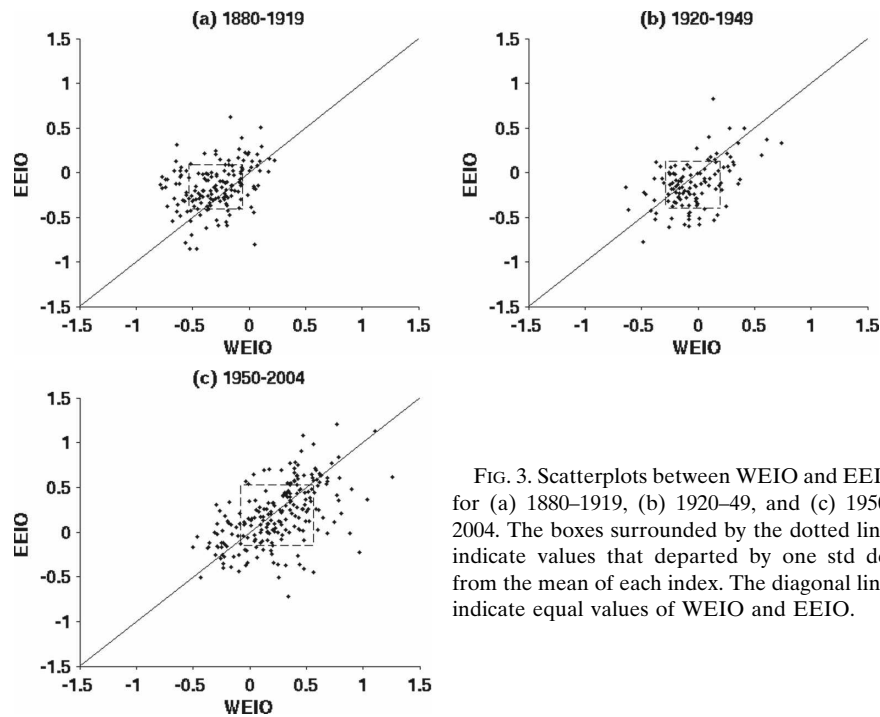


FIG. 3. Scatterplots between WEIO and EEIO for (a) 1880–1919, (b) 1920–49, and (c) 1950–2004. The boxes surrounded by the dotted lines indicate values that departed by one std dev from the mean of each index. The diagonal lines indicate equal values of WEIO and EEIO.

Over the equatorial Indian Ocean, the annual mean winds are weak westerlies and the thermocline depth is relatively flat but larger in the east than in the west (Li et al. 2003). Thus, it is possible to hypothesize that it might take a longer time to warm the upper layer of the eastern equatorial Indian Ocean than the western equatorial Indian Ocean. Also, since WEIO extends farther northward as compared to EEIO, the difference in the timing may arise from the north–south gradient of the warming trend.

b. Relationships between WEIO and EEIO in three periods

Here, we examine the relationship between WEIO and EEIO during the three different warming regimes mentioned in the previous section. Figure 3 shows scatterplots of WEIO versus EEIO averaged over each season: December–February, March–May, June–August, and September–November. These are analyzed separately in the three periods: from 1880 to 1919, from 1920 to 1949, and from 1950 to 2004. Since the scatterplots based on the ERSST and Kaplan SST data exhibit similar patterns, we only show the results based on the ERSST data. The boxes surrounded by the dotted lines indicate values that depart by one standard deviation from the mean of each index. The diagonal lines indicate equal values for WEIO and EEIO. Values that deviate largely from those lines indicate a strong anomalous gradient, that is, a dipole event.

In 1880–1919 (Fig. 3 a), the scatterplot shows a weak relationship between WEIO and EEIO. More data points lie above the diagonal line, implying that WEIO tends to be anomalously colder than EEIO in this period, as we have seen in the time series in Fig. 2. Strong negative dipole events (EEIO much larger than WEIO) that appear as outliers far above the diagonal line occur more frequently than positive dipole events (EEIO much smaller than WEIO) that also appear as outliers far below the diagonal line.

In 1920–49 (Fig. 3b), there is a significant positive relationship between WEIO and EEIO. Compared to the scatterplot for 1880–1919 (Fig. 3a), the box that is surrounded by the dotted lines in Fig. 3b shifts to the right but not up, which could be because of a delayed warming trend over the eastern pole compared to the western one, as we mentioned in the previous section.

The scatterplot for the period, between 1950 and 2004, demonstrates different features from those of the earlier periods (Fig. 3c). The positive connection between WEIO and EEIO appears strong, indicating the intense warming trend that we have seen in the time series of the 10-yr running mean of these SST anomalies. The standard deviations here represent not only natural variability but also the strong trend. Roughly, WEIO and EEIO are evenly scattered above and below the diagonal line. However, unlike scatterplots in the earlier two periods, some extreme outliers where EEIO is much smaller than WEIO are found far below the

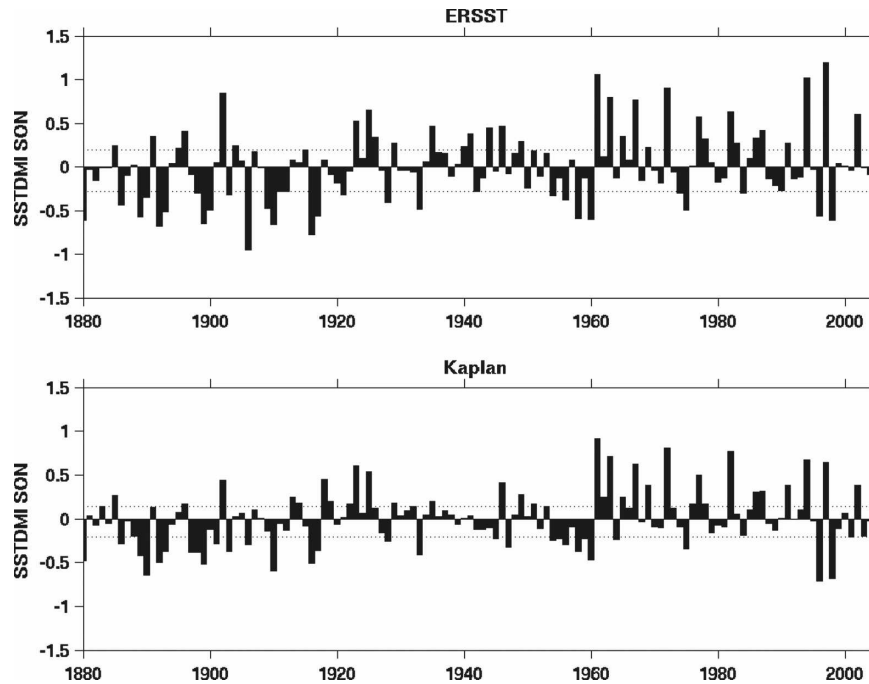


FIG. 4. Time series of September–November SSTDMI from 1880 to 2004: (top) SSTDMI based on ERSST and (bottom) based on the Kaplan SST data. The dotted lines indicate the values of the September–November SSTDMI at the upper and lower 25% of the distribution during the entire analysis period.

diagonal line, reflecting strong anomalous west–east SST gradients over the equatorial Indian Ocean between 1950 and 2004.

The asymmetry in the strong anomalous west–east gradients can be expressed by the skewness of the distribution of WEIO minus EEIO. Positive (negative) skewness implies that the occurrences of strong positive (negative) events are dominant over the occurrences of strong negative (positive) events. The skew coefficient¹ based on the ERSST data is -1.6 in 1880–1919, 0.98 in 1920–49, and 2.3 in 1950–2004. This is consistent with the presence of outliers far above the diagonal line in the scatterplot in 1880–1919 and far below the diagonal line in 1950–2004.

4. Indian Ocean dipole events over the three periods

a. Boreal fall SSTDMI

The Indian Ocean dipole mode index, as derived from SST anomalies (SSTDMI), is obtained by sub-

tracting EEIO from WEIO and represents the anomalous SST gradient between the western equatorial and southeastern regions of the Indian Ocean. The dipole mode also may be represented by other oceanic and atmospheric variables such as zonal wind anomalies, sea level pressure, and the sea surface height of the equatorial Indian Ocean, but in this study, we only examine the index based on SST anomalies that are more reliable than other variables from the earlier period of analysis. Given the changes in the relationship between WEIO and EEIO in the three periods, 1880–1919, 1920–49, and 1950–2004, found in section 3, we expect that the occurrences of the positive and negative dipole mode events have different frequencies in these three periods. As mentioned in the introduction, the Indian Ocean dipole mode has strong seasonal variability (Saji et al. 1999). We take SSTDMI averaged over September–November as the object of our analysis to capture the largest signal of the events.

Figure 4 displays the time series of September–November SSTDMI from 1880 to 2004; the top panel corresponds to the SSTDMI based on the ERSST data and the bottom panel is based on the Kaplan SST data. Overall, SSTDMI based on the Kaplan SST data shows smaller variability. This may be due to the coarser resolution of the Kaplan SST analysis. Two horizontal

¹ The skewness coefficient calculated here is defined as $[1/(N-1)]\sum_{k=1}^N x_k^3/s^3$, where N is the number of the sample, x is WEIO–EEIO, and s is the standard deviation of the sample.

TABLE 1. Individual years when positive dipole mode events occurred in the three periods studied: 1880–1919, 1920–49, and 1950–2004. The positive events are defined as years having September–November SSTDMI values in the upper 25% of the distribution. SSTDMIs based on the ERSST and Kaplan SST data are used to define these years.

1880–1919		1920–49		1950–2004	
ERSST	Kaplan	ERSST	Kaplan	ERSST	Kaplan
1885	1883	1923	1922	1961	1951
1891	1885	1925	1923	1963	1961
1895	1896	1926	1925	1965	1962
1896	1902	1929	1929	1967	1963
1902	1913	1935	1935	1969	1965
1904	1914	1940	1946	1972	1967
1915	1918	1941	1949	1977	1969
	1919	1944		1978	1972
		1946		1982	1976
		1949		1983	1977
				1986	1978
				1987	1982
				1991	1986
				1994	1987
				1997	1991
				2002	1994
					1997
					2002

dashed lines in each figure correspond to the values of September–November SSTDMI at the 25th and 75th percentiles of the distribution over the entire analysis period, 1880–2004, respectively. Meyers et al. (2007) suggested a new method of classifying ENSO and Indian Ocean dipole events that emphasizes the variability over the upwelling regions. However, here we simply define positive (negative) dipole events as having September–November SSTDMI values in the upper (lower) 25% of the distribution during the entire record. Corresponding years of positive and negative events are listed in Tables 1 and 2, respectively.

Between 1880 and 1919, negative events occur more frequently than positive events both in SSTDMI based on the ERSST data and the Kaplan SST data, as pointed out by Kripalani and Kumar (2004) and indicated by our scatterplot of this period (Fig. 3a). In the 1920–49 interval, the magnitude dipole events are smaller compared to the earlier and later periods in both datasets. In the 1950s, the September–November SSTDMI is again in a strong negative phase.

A remarkable transition regarding the strength of the dipole mode events occurs around 1960. After that year, SSTDMIs based on the ERSST and Kaplan SST data display strong and frequent occurrences of the positive dipole mode events in September–November. Some of the positive events (e.g., 1961 and 1997) are so strong that the total SST gradient over the Indian

TABLE 2. Same as in Table 1 but for negative events. The negative events are defined as years having September–November SSTDMI values in the lower 25% of the distribution.

1880–1919		1920–49		1950–2004	
ERSST	Kaplan	ERSST	Kaplan	ERSST	Kaplan
1880	1880	1921	1928	1954	1954
1886	1886	1928	1933	1956	1955
1889	1889	1933	1945	1958	1956
1890	1890	1942	1947	1960	1958
1892	1892			1974	1959
1893	1893			1975	1960
1898	1897			1984	1964
1899	1898			1996	1975
1900	1899			1998	1996
1903	1901				1998
1906	1903				2001
1909	1906				
1910	1910				
1911	1916				
1912	1917				
1916					
1917					

Ocean flips its sign from the climatological gradient and the absolute SST values averaged over the western pole is larger than the absolute SST values averaged over the eastern pole. Negative events do occur in the 1970s and 1990s, but compared to the positive events, the strengths of the negative ones are weak. It appears that during the persistent and strong warming trend after the 1950s, the total SST gradient over the equatorial Indian Ocean, which is usually positive to the east, occasionally flattened.

b. September–November tropical Indo-Pacific SST anomaly patterns during positive and negative dipole events

The main goal in this section is to investigate the Indo-Pacific SST anomaly patterns of the positive and negative dipole events in the three periods including the warming trend and to demonstrate how the meaning of the “dipole” events defined by their index changes with time in terms of the Indo-Pacific SST pattern. As in the previous section, positive (negative) dipole events are defined as having September–November SSTDMI values in the upper (lower) 25% of the distribution during the entire record. The years of positive (negative) events defined by using SSTDMI based on ERSST data are not exactly the same as the years defined by using Kaplan SST data, particularly for the positive events in the periods of 1880–1919 and 1920–49 (Table 1). Around 1915–20 (World War I era) some events are defined as positive in the Kaplan SST data

but not in the ERSST data. Three positive events during 1940–45 (World War II era) are captured by the ERSST data but not by the Kaplan SST data. However, those differences do not substantially impact the main results of this section.

We first confirm the dipole patterns over the Indian Ocean using the mean SST anomalies of each period as the reference state instead of using the entire climatology from 1880 to 2004. In each period the composites of the September–November SST anomalies obtained from the ERSST data over the tropical Indian Ocean during positive–negative events are compared to the composite means including all years of each period, and the difference between them is tested using a two-sample Student's *t* test² (figures not shown). Significant warming compared to the mean of the period over the western pole and significant cooling compared to the mean of the period over the eastern pole are found during positive events in all periods. During negative events significant cooling over the western pole and significant warming over the eastern pole are found in 1880–1919 and 1950–2004, but not in 1920–49. Note that there are only four negative events during this period. Thus, the dipole variability of the positive and negative events is observed in all periods when the different reference states are used in each period. However, when the climatology of the entire period is used as the reference state, what do these same positive and negative events look like?

Figure 5 presents the composites of the September–November SST anomalies over the tropical Indo-Pacific Ocean obtained from the ERSST data during the positive dipole events; the top panel corresponds to the mean in 1880–1919, the middle panel is for 1920–49, and the bottom panel for 1950–2004 (see Table 1 for the individual years). Grid points with values that are significantly different from the zero means³ compared to the 1880–2004 climatology at 95% and higher are shaded.

In 1880–1919 and 1920–49, the eastern pole is colder than normal during the positive dipole events. In 1920–49, the cold anomalies extend over the Maritime Continent and the Southern Hemisphere. In 1880–1919, anomalous warming is observed in the equatorial Pa-

cific. The co-occurrence of the positive Indian Ocean dipole events with El Niños (i.e., a warming anomaly in the eastern equatorial Pacific) is not strong but significant. In 1920–49, there is no significant signal over the tropical Pacific Ocean during positive events except for the small region in the western South Pacific. The time series of SSTDMI and for the Niño-3 region also indicate frequent occurrences of weak positive dipole events in the absence of Pacific warm events in this period (figure not shown). In 1950–2004, during the positive dipole mode events, the western pole tends to be warmer than normal and the eastern pole tends to be colder than normal. It is worth noting that despite the strong warming trend in this period (shown in section 3), the eastern pole still shows significant cooling compared to the climatology during the positive dipole events. A strong warming signal is displayed over the equatorial eastern Pacific Ocean, indicating that strong El Niño events tend to co-occur with positive dipole events during this period (e.g., 1982, 1997). Significant cooling compared to the climatology over the eastern pole is seen during positive events in all three periods, but significant warming compared to the climatology over the western pole appears only in 1950–2004. This can explain why the strength of the positive dipole mode events is dramatically increased after 1960. The same positive events in terms of the dipole mode index exhibit different SST patterns in three periods when the same reference is used. We repeated the same analysis using the Kaplan SST data and obtained similar results, with the El Niño pattern in 1880–1919 composite appearing to be stronger than in the ERSST composites.

Figure 6 is the same as Fig. 5 but during the negative events (see Table 2 for the individual years). In 1880–1919, the Indian Ocean basin is characterized by basin-wide cold anomalies and the absence of significant warmth over the eastern pole. Over the eastern Pacific there are significant cold anomalies, implying that the negative events tends to co-occur with La Niña events. In the 1920–49 interval, there are only four negative events; thus, the statistical significance is not robust enough to judge whether a signal is different from the noise. However, cooling is found over the western pole and warming is found over the eastern pole. La Niña features are seen in the Pacific basin although they are not significant at the 95% level. In 1950–2004, over the Indian Ocean, the eastern pole is warmer than normal and the southern Indian Ocean is colder than normal, but there is no signal at the western pole. Over the equatorial Pacific Ocean, there is weak but significant cooling. We obtained the same results using the Kaplan SST data. However, in 1950–2004, significant cooling over the southern Indian Ocean is not found and the La

² The test statistics of the two-sample Student's *t* test is $(\mu_1 - \mu_2) / \sqrt{(s_1^2/n_1 + s_2^2/n_2)}$, where μ_1 and μ_2 are the means, s_1 and s_2 the standard deviations of samples 1 and 2, and n_1 and n_2 are the numbers of values in samples 1 and 2, respectively.

³ The test statistics of the Student's *t* test is obtained by $\mu / \sqrt{(s^2/n)}$, where μ is the mean of the sample, s is the standard deviation of the sample, and n is the number of the sample. It is calculated using the mean, standard deviation, and sample number of each period. A two-tailed test is used in this analysis.

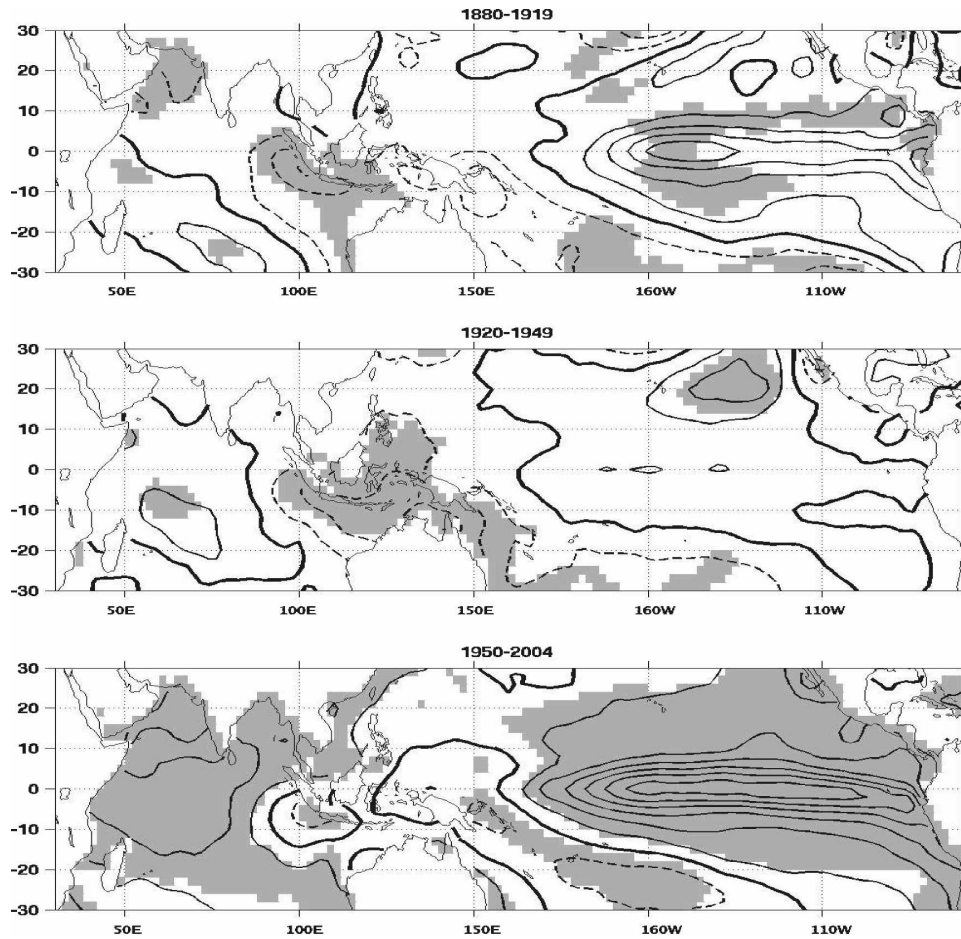


FIG. 5. Composites of September–November SST anomalies over the tropical Indo-Pacific Ocean during the positive dipole events: mean in (top) the 1880–1919, (middle) 1920–49, and (bottom) 1959–2004. Grid boxes that are significantly different from zero means, i.e., climatological mean of the period between 1880 and 2004, using a Student's t test at the 95% level and higher are shaded. The positive events are defined as years having September–November SSTDMI values in the upper 25% of the distribution. The solid lines correspond to the positive values, the dashed lines to the negative values, and the thick lines to zero. The contour interval is 0.2°C .

Niña signal over the Pacific is stronger than that in the ERSST data.

5. Summary and discussions

The state of the Indian Ocean dipole mode is investigated using SST anomaly data from 1880 to 2004. The SST anomalies over the western and eastern poles of the Indian Ocean dipole show a clear warming trend during the entire period of analysis, particularly after the 1950s. The warming trend appears in the western pole around the 1910s, about a decade earlier than in the eastern pole in both the ERSST and Kaplan SST datasets, which were reconstructed by different methods, although the limitation of the quality in the historical SST data disallows a precise discussion on this

issue. The relationship between the SST anomalies averaged over the western pole of the dipole, WEIO, and the SST anomalies averaged over the eastern pole, EEIO, shows different features in the earlier period compared to the later period. In 1880–1919, WEIO tends to be anomalously colder than EEIO most of the time. Whereas in 1950–2004, the values in the WEIO are generally comparable to the values in the EEIO. However, the existences of occasional outliers where WEIO is anomalously much warmer than EEIO stand out.

In 1880–1919, more negative Indian Ocean dipole events occur in September–November than positive events. In 1920–49, some positive events occur in the ERSST data but these events are weak. Few negative events occur in this period. Strong and frequent posi-

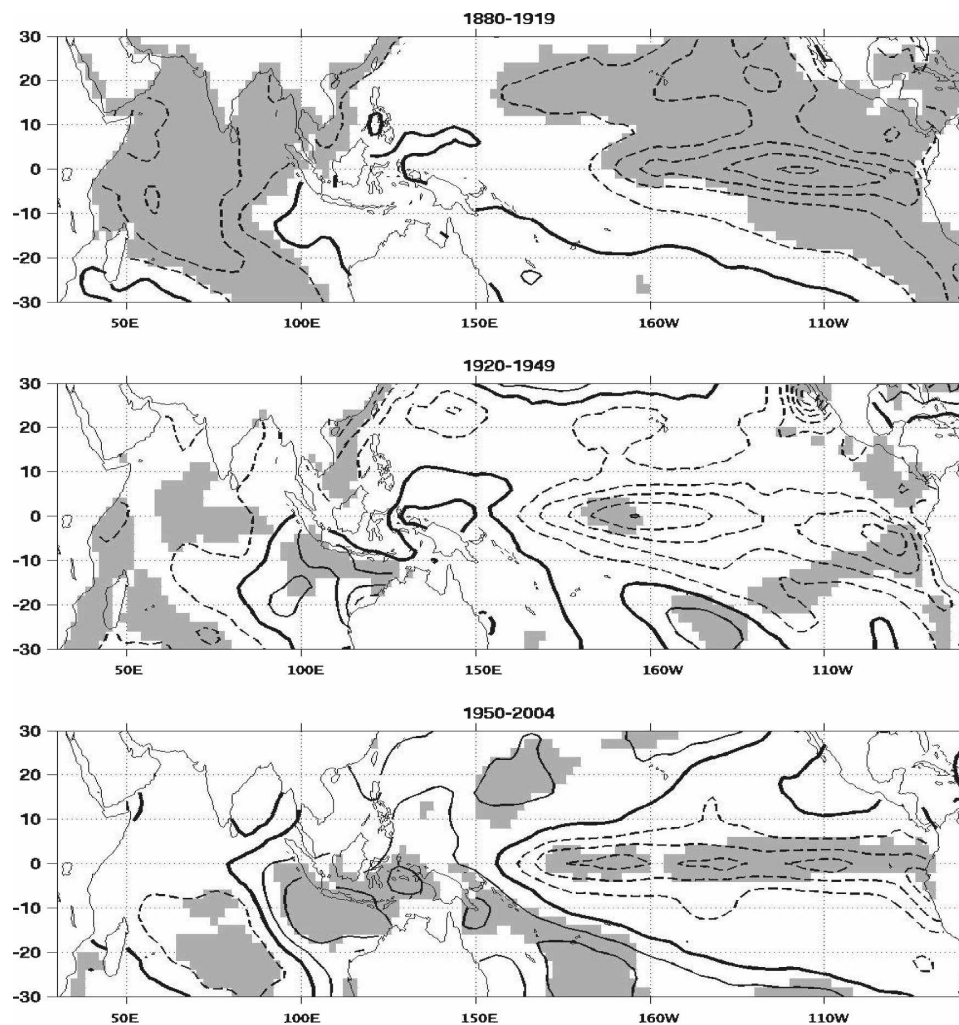


FIG. 6. Same as in Fig. 5, but for the negative events. The negative events are defined as years having September–November SSTDMI values in the lower 25% of the distribution during the entire period.

tive events appear after 1960. These positive events are characterized by both significant anomalous warming over the western pole and significant anomalous cooling over the eastern pole, whereas only significant cooling compared to the climatology over the eastern pole is observed in the earlier two periods. With respect to the association with Pacific events, positive dipole mode events are strongly significantly linked with El Niño events in 1950–2004 and negative events with La Niña events in 1880–1919. Two different historical SST reconstructions are used in this study, but overall our results are not sensitive to which SST datasets are used.

There is ongoing debate in the research community regarding whether the Indian Ocean dipole mode is a phenomenon that is independent of ENSO. Our composites maps of Indo-Pacific SST anomalies during positive (negative) events demonstrate a strong El Niño

(La Niña) signal over the Pacific during the period between 1950 and 2004 (1880 and 1919). At the same time, analyses of observational data from the late nineteenth century to the present performed in this paper and in Ashok et al. (2003), as well as some modeling work (Behera et al. 2006; Bracco et al. 2005; Lau and Nath 2004; Fischer et al. 2004), indicate that the dipole events can sometimes occur without ENSO. Some weak positive events in 1920–49 are examples. Also, the results presented in this paper make us speculate that the dipole mode events in the early twentieth century are influenced by the warming trend that started over this region during that period. In 1880–1919, before the appearance of the strong warming trend over this region, WEIO tended to be anomalously colder than EEIO most of the time, and thus we see the strong negative events show in Fig. 4, since we have used the

climatology of the entire period from 1880 to 2004 as the reference. It can be said that the warming trend appeared earlier in WEIO than in EEIO; thus, the values of WEIO caught up with those of EEIO before the warming trend started over EEIO. After the 1960s, unlike in the early twentieth century, the values of WEIO are mostly comparable to those of EEIO. However, strong positive events that are characterized by both significantly warmer than normal WEIO and significantly colder than normal EEIO occasionally appear; something that is not found in the earlier two periods.

It is interesting that the eastern pole sometimes cools among the strong warming trend over this region. In contrast to the surface warming trend of the Indian Ocean, Alory et al. (2007) found a subsurface cooling trend of the main thermocline over the Indonesian Throughflow region, that is, near EEIO, in 1960–99, the interval using the new Indian Ocean Thermal Archive. Thus, it can be speculated that water carried to the surface by upwelling during positive dipole events is becoming colder and results in a colder EEIO during positive events in recent decades. We also hypothesize that shoaling of the thermocline over the EEIO, corresponding to a subsurface cooling trend (Alory et al. 2007), can make this region more susceptible to the wind–thermocline feedback and leads to frequent occurrences of positive events in recent decades. Thus, the emergence of intense and frequent positive dipole events in recent decades may be speculated to have some connection to the trend of the climatic conditions over this region.

Acknowledgments. Authors offer their thanks to Dr. Alexey Kaplan for helpful comments on the datasets. This work was supported by NASA Headquarters under Earth System Science Fellowship Grant NGT5. Both YK and MAC were supported under NSF Grant ATM0347009.

REFERENCES

- Allan, R. J., J. A. Lindesay, and C. J. C. Reason, 1995: Multidecadal variability in the climate system over the Indian Ocean region during the austral summer. *J. Climate*, **8**, 1853–1873.
- , and Coauthors, 2001: Is there an Indian Ocean dipole, and is it independent of the El Niño–Southern Oscillation? *CLIVAR Exchanges*, Vol. 6, No. 3, International CLIVAR Project Office, Southampton, United Kingdom, 18–22.
- Alory, G., S. Wijffels, and G. Meyers, 2007: Observed temperature trends in the Indian Ocean over 1960–1999 and associated mechanisms. *Geophys. Res. Lett.*, **34**, L02606, doi:10.1029/2006GL028044.
- Annamalai, H., J. Potemra, R. Murtugudde, and J. P. McCreary, 2005: Effect of preconditioning on the extreme climate events in the tropical Indian Ocean. *J. Climate*, **18**, 3450–3469.
- Ashok, K., Z. Guan, and T. Yamagata, 2001: Impact on the Indian Ocean dipole on the relationship between the Indian monsoon rainfall and ENSO. *Geophys. Res. Lett.*, **28**, 4499–4502.
- , —, and —, 2003: A look at the relationship between the ENSO and the Indian Ocean dipole. *J. Meteor. Soc. Japan*, **81**, 41–56.
- , W. Chan, T. Motoi, and T. Yamagata, 2004a: Decadal variability of the Indian Ocean dipole. *Geophys. Res. Lett.*, **31**, L24207, doi:10.1029/2004GL021345.
- , Z. Guan, N. H. Saji, and T. Yamagata, 2004b: Individual and combined influences of the ENSO and the Indian Ocean dipole on the Indian summer monsoon. *J. Climate*, **17**, 3141–3154.
- Behera, S. K., J. J. Luo, S. Masson, P. Delecluse, S. Gualdi, A. Navarra, and T. Yamagata, 2005: Paramount impact of the Indian Ocean dipole on the East African short rains: A CGCM study. *J. Climate*, **18**, 4514–4530.
- , —, —, S. A. Rao, H. Sakuma, and T. Yamagata, 2006: A CGCM study on the interaction between IOD and ENSO. *J. Climate*, **19**, 1688–1705.
- Bracco, A., F. Kucharski, F. Molteni, W. Hazeleger, and C. Severijns, 2005: Internal and forced modes of variability in the Indian Ocean. *Geophys. Res. Lett.*, **32**, L12707, doi:10.1029/2005GL023154.
- Chang, P., and Coauthors, 2006: Climate fluctuations of tropical coupled system—The role of ocean dynamics. *J. Climate*, **19**, 5122–5174.
- Clark, C. O., P. J. Webster, and J. E. Cole, 2003: Interdecadal variability of the relationship between the Indian Ocean zonal mode and East African coastal rainfall anomalies. *J. Climate*, **16**, 548–554.
- Fischer, A. S., P. Terray, E. Guilyardi, S. Gualdi, and P. Delecluse, 2004: Two independent triggers for the Indian Ocean dipole/zonal mode in a coupled GCM. *J. Climate*, **18**, 3428–3449.
- Guan, Z., and T. Yamagata, 2003: The unusual summer of 1994 in East Asia: IOD teleconnections. *Geophys. Res. Lett.*, **30**, 1544, doi:10.1029/2002GL016831.
- Hurrell, J. W., and K. E. Trenberth, 1999: Global sea surface temperature analyses: Multiple problems and their implications for climate analysis, modeling, and reanalysis. *Bull. Amer. Meteor. Soc.*, **80**, 2661–2678.
- Ihara, C., Y. Kushnir, and M. A. Cane, 2008: July droughts over the homogeneous Indian monsoon region and Indian Ocean dipole during El Niño events. *Int. J. Climatol.*, in press.
- Jones, P. D., D. E. Parker, T. J. Osborn, and K. R. Briffa, 2006: Global and hemispheric temperature anomalies—Land and marine instrumental records. *Trends: A Compendium of Data on Global Change*, Carbon Dioxide Information Analysis Center, Oak Ridge National Laboratory, U.S. Department of Energy, Oak Ridge, TN.
- Kaplan, A., M. Cane, Y. Kushnir, A. Clement, M. Blumenthal, and B. Rajagopalan, 1998: Analyses of global sea surface temperature 1856–1991. *J. Geophys. Res.*, **103**, 18 567–18 589.
- , M. A. Cane, and Y. Kushnir, 2003: Reduced space approach to the optimal analysis interpolation of historical marine observations: Accomplishments, difficulties, and prospects. Advances in the Applications of Marine Climatology: The Dynamic Part of the WMO Guide to the Applications of Marine Climatology, WMO/TD-1081, World Meteorological Organization, Geneva, Switzerland, 199–216.
- Kripalani, R. H., and P. Kumar, 2004: Northeast monsoon rainfall variability over south peninsular India vis-à-vis the Indian Ocean dipole mode. *Int. J. Climatol.*, **24**, 1267–1282.

- , J. H. Oh, J. H. Kang, S. S. Sabade, and A. Kulkarni, 2005: Extreme monsoons over East Asia: Possible role of Indian Ocean zonal mode. *Theor. Appl. Climatol.*, **82**, 81–94.
- Kulkarni, A., S. S. Sabade, and R. H. Kripalani, 2007: Association between extreme monsoons and the dipole mode over the Indian subcontinent. *Meteor. Atmos. Phys.*, **95**, 255–268.
- Lau, N.-C., and M. J. Nath, 2004: Coupled GCM simulation of atmosphere–ocean variability associated with zonally asymmetric SST changes in the tropical Indian Ocean. *J. Climate*, **17**, 245–265.
- Li, T., B. Wang, C.-P. Chang, and Y. S. Zhang, 2003: A theory for the Indian Ocean dipole–zonal mode. *J. Atmos. Sci.*, **60**, 2119–2135.
- Meyers, G., P. McIntosh, L. Pigot, and M. Pook, 2007: The years of El Niño, La Niña, and interactions with the tropical Indian Ocean. *J. Climate*, **20**, 2872–2880.
- Reverdin, G., D. L. Cadet, and D. Gutzler, 1986: Interannual displacements of convection and surface circulation over the equatorial Indian Ocean. *Quart. J. Roy. Meteor. Soc.*, **112**, 43–67.
- Saha, K., 1970: Zonal anomaly of sea surface temperature in equatorial Indian Ocean and its possible effect upon monsoon circulation. *Tellus*, **4**, 403–409.
- Saji, N. H., and T. Yamagata, 2003: Possible impacts of Indian Ocean dipole mode events on global climate. *Climate Res.*, **25**, 151–169.
- , B. N. Goswami, P. N. Vinayachandran, and T. Yamagata, 1999: A dipole mode in the tropical Indian Ocean. *Nature*, **401**, 360–363.
- Slutz, R. J., S. J. Lubker, J. D. Hiscox, S. D. Woodruff, R. L. Jenne, D. H. Joseph, P. M. Steuer, and J. D. Elms, 1985: Comprehensive Ocean–Atmosphere Data Set: Release 1. NOAA/Environmental Research Laboratories/Climate Research Program, Boulder, CO, 268 pp. [NTIS PB86-105723.]
- Smith, T. M., and R. W. Reynolds, 2003: Extended reconstruction of global sea surface temperatures based on COADS data (1854–1997). *J. Climate*, **16**, 1495–1510.
- , and —, 2004: Improved extended reconstruction of SST (1854–1997). *J. Climate*, **17**, 2466–2477.
- Terray, P., and S. Dominiak, 2005: Indian Ocean sea surface temperature and El Niño–Southern Oscillation: A new perspective. *J. Climate*, **18**, 1351–1368.
- Tozuka, T., J. J. Luo, S. Masson, and T. Yamagata, 2007: Decadal modulations of the Indian Ocean dipole in the SINTEX-F1 coupled GCM. *J. Climate*, **20**, 2881–2894.
- Webster, P. J., A. M. Moore, J. P. Loschnigg, and R. R. Leben, 1999: Coupled ocean–atmosphere dynamics in the Indian Ocean during 1997–98. *Nature*, **401**, 356–360.